Aalborg Universitet

"Active flux" orientation vector sensorless control of IPMSM

Blaabjerg, Frede; Boldea, I.; Paicu, M.C.; Andreescu, G.D.

"Active Flux" Orientation Vector Sensorless Control of IPMSM

Ion Boldea[*], *Fellow, IEEE,* Mihaela Codruta Paicu[*], Gheorghe Daniel Andreescu[**], *Senior Member, IEEE,* Frede Blaabjerg[***], *Fellow, IEEE*

[*]Dept. of Electrical Engineering, [**]Dept. of Automation and Applied Informatics,
University Politehnica of Timisoara, 2 Vasile Parvan Blvd., 300223 Timisoara, Romania
email: boldea@lselinux.utt.ro, paicucodruta@yahoo.com, daniel.andreescu@aut.upt.ro
[***]Institute of Energy Technology, Aalborg University, 101 Pontoppidanstraede, 9220 Aalborg East, Denmark
email: fbl@iet.aau.dk

Abstract—**This paper presents a novel strategy for the vector control of IPMSM, without signal injection. The overall performance of the motion-sensorless control depends strongly on the accuracy of the rotor position and speed estimation. The proposed state observer is based on the concept of the "active flux" (or "torque producing flux"), which "turns all the salient–pole rotor ac machines into nonsalient–pole ones". As well as giving a detailed explanation of the concept, the paper demonstrates, through a wide range of experimental results, the effectiveness of the active flux observer under half full rated torque operating conditions in 2 rpm-1000 rpm speed range.**

Keywords—**active flux observer, sensorless control, low speed operation, vector control.**

I. INTRODUCTION

In the ac control drives, adoption of motors of IPMSM type is continuously increasing.

More over, in the last few years the search for position sensorless control has emerged, thus involving very low or even zero speed operation [1]-[8].

The methods for sensorless position estimation can be divided into two main categories: approaches using back-electromotive-force (EMF) estimation with fundamental excitation and spatial saliency image tracking methods using excitation in addition to the fundamental. The saliency tracking methods [9]-[15] are suitable for zero-speed operation, whereas the back-EMF-based methods fail at low speed [16]-[19].

In the saliency and signal injection methods, the feature of a salient-pole PMSM such that the inductance varies depending on the rotor position is used to estimate the rotor position. Such methods suppose a high frequency voltage or current injected signal from the inverter in order to detect inductance variation. Thus, the position can be estimated even at standstill and low-speeds by these methods.

On the other hand, the fundamental excitation method does not need any additional signal, but does not operate at zero speed. There are a lot of different estimation methods in this category. Some of them, using the Kalman filter, MRAC [20] or the INFORM method [21] allow low and zero speed operation, but are apparently too complex and expensive to be used in practical systems. Other methods extract rotor flux information from measured electrical quantities, especially from stator voltage and stator current. However, it is quite critical to estimate position at low speed region, since the flux signals are contaminated by noises, stator resistance variation with temperature, DC-offset and drifting terms in the feedback currents [1], [14].

The sensorless strategy implemented in this paper belongs to this fundamental excitation method and it is based on the concept of the "active flux" (or "torque producing flux"), which "turns all the salient–pole machines into nonsalient–pole ones". Its main advantage is that the proposed sensorless technique can be applied to universal ac drives. The "active flux" concept was developed in [19], [7] and [8].

This paper is focused on rotor position and speed estimation of IPMSM from a new "active flux" observer, in order to achieve very low speed operation.

The implemented active flux based observer ensures proper motion-sensorless operation down to 2 rpm with half full rated torque, without signal injection.

Experimental results demonstrate the performance of the active flux observer under steady-state and transient conditions.

II. THE ACTIVE FLUX CONCEPT

The "active flux" concept, as developed in [7], turns all salient - pole - rotor ac machines into fictitious nonsalient-pole machine such that the rotor position and speed estimation become simpler.

Let us briefly define the active flux $\overline{\psi}_d^a$ as the flux that multiplies i_q in the *dq*-model torque expression of all ac machines.

$$T_e = \frac{3}{2} p_1 \psi_d^{\ a} i_q \qquad (1)$$

with: $\qquad \psi_d^{\ a} = \psi_{PMd} + \left(L_d - L_q\right)i_d \, ; \ L_d < L_q \qquad (2)$

for IPMSM in which case, axis d corresponds to the rotor pole axis. L_d, L_q are the *dq* inductances, ψ_{PMd} is the PM flux linkage.

As demonstrated in [7], $\overline{\psi}_d^a$ represents the torque producing flux and then the model of IPMSM "looses" magnetic anisotropy and manifests itself by the inductance L_q (torque current is i_q as in (1)):

$$\overline{V}_s^s = R_s \overline{i}_s^s + (s + jw_1)L_q \overline{i}_s^s + (s + jw_1)\overline{\psi}_d^{as} \qquad (3)$$
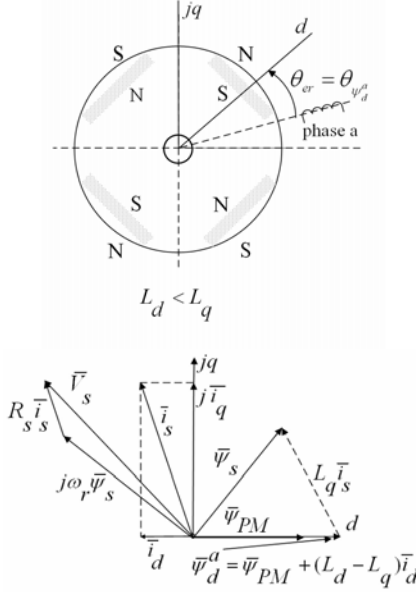
Figure 1.IPMSM and its vector diagram pointing out the active flux $\bar{\psi}_d^a$

The derivation of (3), from the *dq* model of IPMSM is straightforward.

To explicit the concept quickly, the steady state vector diagram with $\bar{\psi}_d^a$ in foreground is drawn in Figure 1.

The space phasor stator voltage equation in stator coordinates:

$$\bar{V}_s^s = R_s \bar{i}_s + \frac{d\bar{\psi}_s}{dt} \qquad (4)$$

By definition, the active flux vector $\bar{\psi}_d^a$ observer, in stator coordinates, is:

$$\bar{\psi}_d^{as} = \int (\bar{V}_s - R_s \bar{i}_s + V_{comp})dt - L_q \bar{i}_s^s \qquad (5)$$

$\bar{\psi}_d^{as}$ axis falls along rotor axis d and thus:

$$\bar{\psi}_d^{as} = \psi_d^a cos\theta_{\psi_d^a} + j\psi_d^a sin\theta_{\psi_d^a} \qquad (6)$$

V_{comp} is compensating the various errors in the $\bar{\psi}_d^{as}$ estimation as inverter nonlinearities (power switch voltage drop, dead-time), integration dc-offset, stator resistance correction, magnetic saturation.

The active flux observer (5) is practically the same in structure for all ac machines. It leads to the estimation of both ψ_d^a amplitude and angle $\theta_{\psi_d^a}$ with respect to stator phase a ($\theta_{\psi_d^a} = \theta_{er}$) for PMSMs.

To provide decoupled torque control, ψ_d^a should be kept rather constant up to based speed.

III. VECTOR CONTROL SYSTEM

Figure 2 illustrates the proposed vector control system for IPMSM, which consists in space vector modulator block (SVM), vector control implementation scheme, active flux observer and rotor position-speed estimator.

The SVM block, whose technique includes dead time and nonlinearities compensation, generates the switching signals for the voltage source inverter.

The vector control system uses the voltage model (4) in stator flux reference.

To obtain a smooth speed reference signal and to avoid the overshooting a PT1 filter based on the following relation is implemented:

$$\frac{k_{PT1}}{(T_{PT1} \cdot s + 1)} \qquad (7)$$

where, for our case: $k_{pw\_PT1}=1$, $T_{iw\_PT1}=0.025$.

The speed controller is of PI type with anti-windup and torque limiter. Its proportional gain is $k_{pw}=0.1$ and the integral gain is $k_{iw}=20$ (Figure 2).

In the vector control scheme accurate speed control depends on how well the current vector is regulated.

Most of the reported work on control of IPMSM took an assumption of $i_d = 0$ in order to simplify the development of the controller.

The two PI current control loops have been implemented in a synchronous rotating *dq* reference frame having a better performance than stationary frame regulators, as they operate on dc quantities and hence can eliminate steady-state errors.

The controllers are started from zero initial states, thus the scheme gives a meaningful estimate right away.

The design of the current controller employs the relation (Figure 2):

$$k_p(1+\frac{k_i}{s}) \qquad (8)$$

The proportional and integral gains for the PI controller on the *d* axis are $k_{pd}=50$, $k_{id}=100$, respectively for the PI controller on the *q* axis $k_{pq}=30$, $k_{iq}=100$ and were chosen by trial and error for the IPMSM with the data in Table 1.

The output voltages (V_d^*, V_q^*) are compensated (by motion emfs $V_{d\_decoupling}$ and $V_{q\_decoupling}$) in order to eliminate the cross coupling between *d* and *q* axis.

Even more, V_d^* and V_q^* should satisfy the following limit to avoid the voltage saturation:

$$V_d^{*2} + V_q^{*2} \leq V_{max}^2 \qquad (9)$$

The maximum stator voltage V_{max} is determined from the available dc-link voltage V_{dc} and pulse width modulation (PWM) strategy (in our case space vector modulation (SVM)) and thus $V_{max} = \frac{V_{dc}}{\sqrt{3}}$.
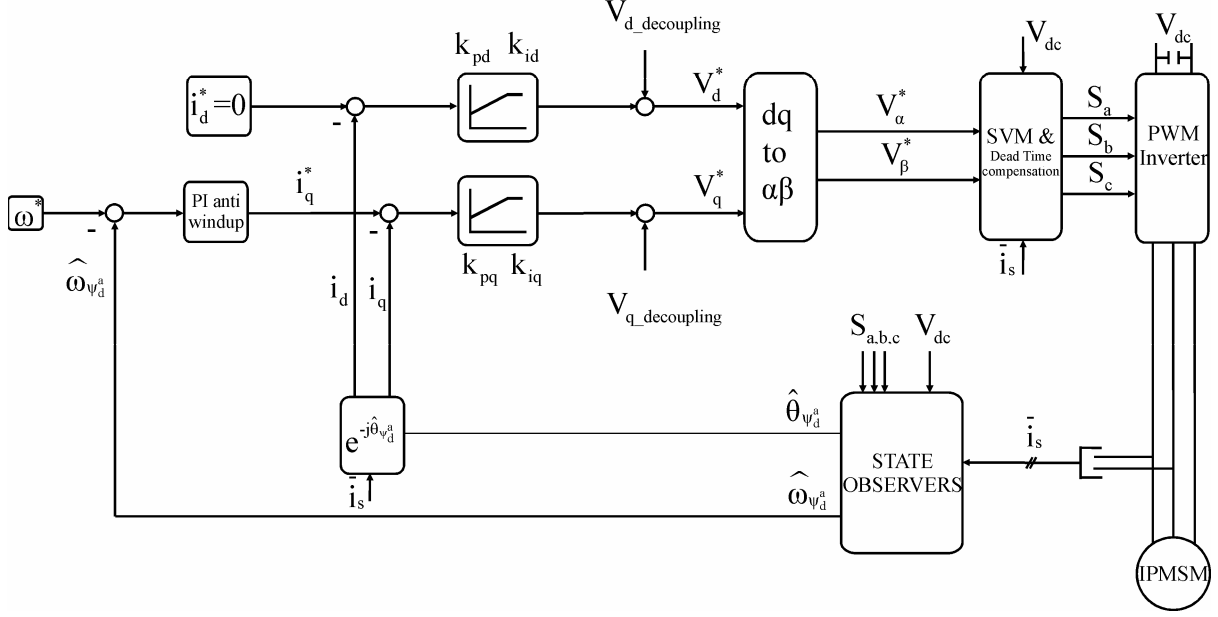
Figure 2. The proposed vector control system for IPMSM

The voltage drop on the power devices of the inverter has to be subtracting from the dc-link voltage when operating at low frequency (low voltage amplitude), otherwise distortion and discontinuities in the voltage waveform.

The main block of the proposed sensorless algorithm is the rotor position estimator, which makes the difference from the standard sensor-used vector control system.

The position estimator produces two filtered estimates of the rotor position (in this case the active flux rotor position $\hat{\theta}_{\psi_d^a}$) and the electrical speed $\hat{\omega}_{\psi_d^a}$ from the two inputs of the stator-current ($\bar{i}_s$) and stator-voltage command in the stationary reference frame (V_α^*, V_β^*). Instead of its command, the actual voltage can be used at the cost of additional hardware. By using the implementation of the space vector modulator (SVM), the voltage generated by the inverter system closely corresponds to the voltage command from the current regulator. The terminal-voltage measurement is, therefore, not required and the voltage command can be used successfully as voltage information. Of course, to generate precise terminal voltage according to the command, the dc-link voltage information should be available and the sensing equipment for link voltage is required.

In practical use, the estimated speed $\hat{\omega}_{\psi_d^a}$ is filtered through a low-pass filter to reduce the influence of noise. The filtered estimated speed is then used in the control system.

The estimated angle $\hat{\theta}_{\psi_d^a}$ was used for supplying all vector transformations between the *abc* and *dq* frames.

In the proposed control system, a startup procedure ensures that the estimated position and speed operate properly at startup. This procedure consists in forcing the rotor in a known home position and is achieved by triggering the proper voltage vector ($\bar{V}_1(1,0,0)$).

The known rotor position is now taken into consideration by the integrator from the flux observer.

This completes the general description of the proposed sensorless vector control system in Figure 2.

IV. THE STATE OBSERVERS

A. The Active Flux Observer

The state observer has to be the fastest element in the sensorless control scheme.

The operating principle for this observer is to extract the active flux information by measuring the stator voltages and currents.

In fact the dc voltage is measured and the inverter state current is used to "construct" the ac stator voltage waveforms.

The active flux observer implementation scheme is presented in Figure 4 and it consists in a stator flux observer in stator coordinates from which the term $L_q i_s$ is subtracted (5).
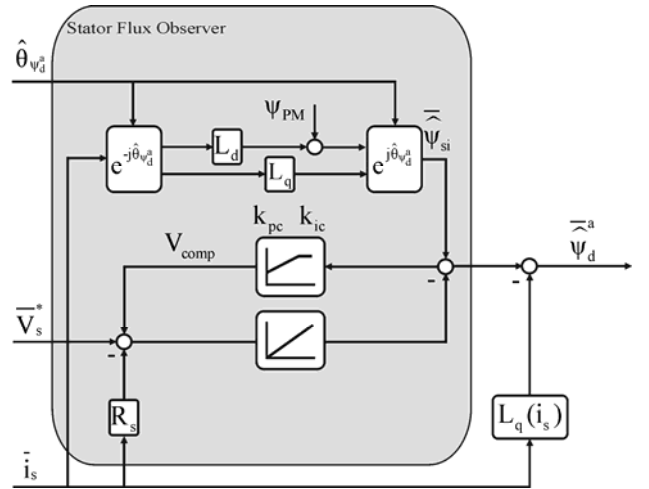

Figure 3. The stator flux observer

The stator flux observer combines advantages of the current model (including magnetic saturation) at low speed with the voltage model at medium-high speed, using a compensation loop driven by the current estimation error.

The voltage compensation employs the following equation, as it can be observed in Figure 3:

$$V_{comp} = (k_p + \frac{k_i}{s})(\overline{\psi}_{si} - \overline{\psi}_{su}) \qquad (10)$$

The proportional and integral gains for the compensation PI term (k_{pc}=4, k_{ic}=4) were also chosen by trial and error method.

The accuracy of active flux estimation is very limited at low speed due to noise, DC-offset and drifting terms in the feedback currents and stator resistance variation, which deviates from its nominal value.

The noise is decreased by filtering the feedback signal of the rotor speed estimation.

To eliminate the DC-offset and drifts from the voltage integration circuits and the current feedback, a low pass filter (LPF) is used in [1].

However, in the practical control system, a pure integrator was used. Thus the usual estimation errors associated with using a LPF (the lag in the signals processing) are avoided, which is very important when operating at very low speed.

The observer is sensitive to the stator resistance error, especially at low speeds when the back electromotive force (EMF) decreases and the stator resistance voltage drop becomes significant. Thus, any small error in the stator resistance (due to the variation with the temperature) perturbs the stator flux estimation and implicitly the active flux estimation. A compensation method was detailed in [2].

In the experimental tests the stator resistance value was set to $R_s = 4\Omega$ (hot temperature value).

However, V_{comp} also compensates the errors in the stator flux estimation, occurred due to the inverter nonlinearities, stator resistance variation, integration offset and magnetic saturation.

B. The Position-Speed Estimator

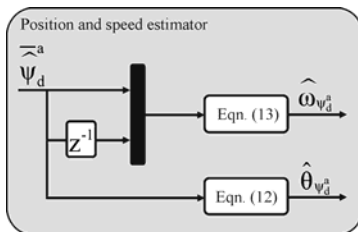The rotor position-speed estimator implementation is illustrated in Figure 4.

Figure 4. The position-speed observer

Usually a PLL (phase-locked-loop) estimator is used for rotor position-speed estimation. In what follows, however we make use of the estimator in (11)-(13)below:

$$\hat{\omega}_{\psi_d^a} = \frac{d\hat{\theta}_{\psi_d^a}}{dt} \qquad (11)$$

$$\hat{\theta}_{\psi_d^a} = \text{atan}(\frac{\psi_{d\beta}^a}{\psi_{d\alpha}^a}) \qquad (12)$$

$$\hat{\omega}_{\psi_d^a} = \frac{\psi_{d\alpha k-1}^a \psi_{d\beta}^a - \psi_{d\beta k-1}^a \psi_{d\alpha}^a}{h(\psi_{d\alpha}^{a\,2} + \psi_{d\beta}^{a\,2})} \qquad (13)$$

The rotor speed estimation $\hat{\omega}_{\psi_d^a}$ in the whole speed range is required in the speed controller. A low pass filter is applied to the estimated speed to reduce the noise.

This filter is a PT1, where the proportional gain is k_{p_PT1}=1, respectively the integral gain is T_{i_PT1}=0.003.

The transformations between the reference frames in both feedforward and feedback paths in Figure 2 can be affected by inaccurate rotor position estimation. Position estimation errors will be thoroughly checked.

V. EXPERIMENTAL PLATFORM AND TEST RESULTS

The proposed sensorless vector control has been validated on the experimental prototype with the data presented in Table 1. This was possible by developing the system control algorithm in MATLAB/Simulink, followed by its implementation on a dSpace PPC 1103 controller board.

TABLE 1.
PARAMETERS OF THE PROTOTYPE IPMSM

Number of pole pairs (p)	3
Rated power	2.2 kW
Rated speed	1750 rpm
Rated frequency	87.5 Hz
Rated torque	12 Nm
Rated phase to phase voltage	380 V(rms)
Rated phase current	4.1 A(rms)
Stator resistance per phase (Rs)	3.3 Ω
d-axis inductance (Ld)	41.59 mH
q-axis inductance (Lq)	57.06 mH
Rotor permanent - magnet (λPM)	0.4832 V s rad-1
Inertia of the rotating system (J)	10.07x10-3 kgm2
Viscous friction coefficient (Bm)	20.44x10-4Nms/rad

Figure 5 illustrates a three phase, 2.2kW IPMSM, which is directly coupled to the load machine (Siemens PMSM), speed controlled by separated frequency inverter (Siemens SIMOVERT MASTERDRIVE).

A three phase IGBT inverter, supplied at a dc link voltage of 540V, fed the IPMSM. The sampling frequency and PWM frequency are set to 10 kHz. The dead time of the inverter is set to 2 μs. All three phase currents are measured using magnetic current transducers. A dSpace PPC 1103 controller board interfaces the three current sensors.

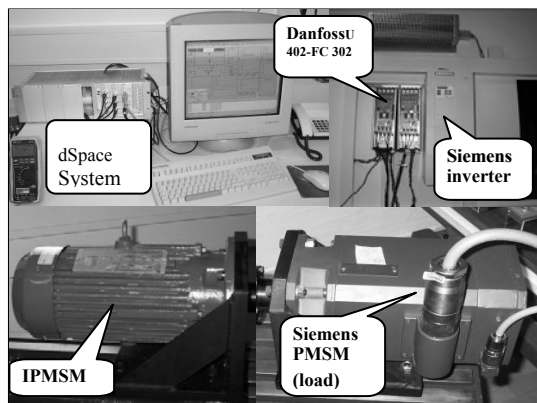The actual rotor position and speed are provided by an incremental encoder with 2048 pulses per revolution.

Figure 5. Experimental setup

Experimentally it has been observed that the control was sensitive to the dead time compensation (because of dead time influence, the voltage applied to the machine was lower than the one commanded) and to the stator resistance, especially at low speeds.

The startup procedure is mandatory and it aligns the machine, by giving the proper voltage vector.

It has been observed that when the speed reference or load torque changes rapidly, a position (speed) estimation error occurs.

The following test runs have been performed to check the proposed concept:

a. Steady state operation at lowest speed (2 rpm) and 50% rated torque (Figure 6)

b. Step speed reduction from 5 rpm to 3 rpm at 50% rated torque (Figure 7)

c. Steady state operation at 5 rpm and 100% rated torque (Figure 8)

d. ± 15 rpm speed reversal at 50% rated torque (Figure 9)

e. Step nominal rated torque response at 20 rpm (Figure 10)

f. Startup response from zero to 1000 rpm, followed by ± 1000 rpm speed reversal plus 60% step torque loading response (Figure 11)

The lowest speed achieved with the implemented sensorless control system is 2 rpm, operating under a step disturbance of 50% rated torque.

The rotor position estimation errors are notable, but acceptable. The estimated angle rotor position fluctuates around actual one. The fluctuation causes small current distortion and speed variation.

Further improvements in position estimation precision are both necessary and feasible.

The presented speed-reversal results in Figure 9 show a good transition through zero speed.

The rotor position estimation error and the rotor speed estimation error increase when the speed reference or load disturbance change quickly, as it is shown in Figs. 9, 10, 11. Also during steady state the rotor speed estimation errors are less than 7-13 rpm, during transients they go up to 50 rpm.
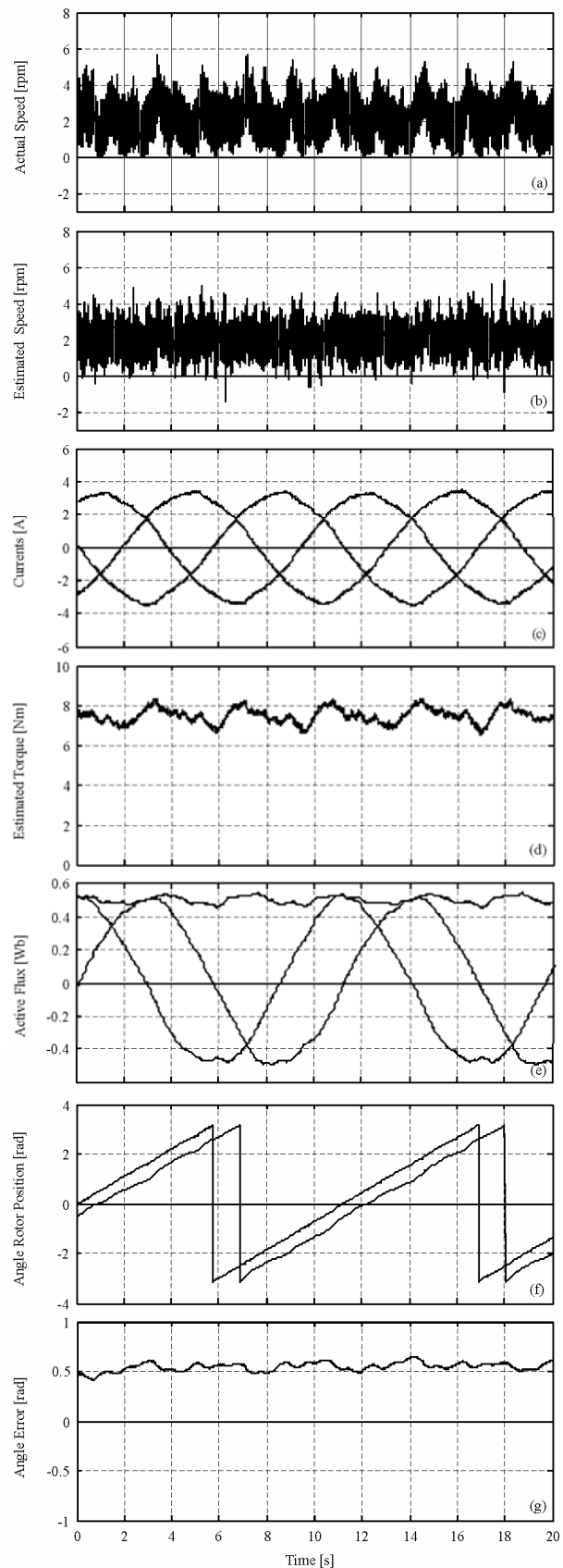

Figure 6. Steady state sensorless operation at lowest speed of 2 rpm (0.1Hz) and 50% of nominal torque; from top to bottom: actual speed, estimated speed, measured currents, estimated torque, active flux, angle rotor position (actual and estimated), error between estimated and actual angle rotor position
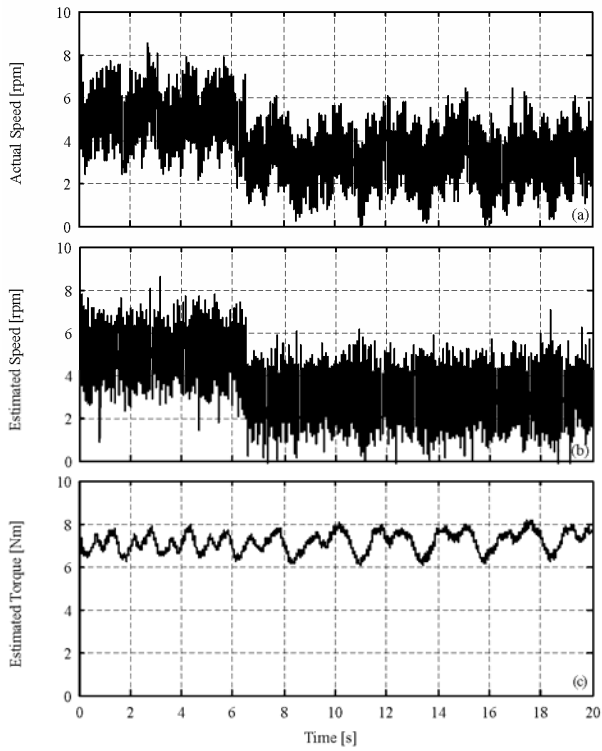
Figure 7. Transients from 5 rpm to 3 rpm at 50% of nominal torque; from top to bottom: actual speed, estimated speed and estimated torque
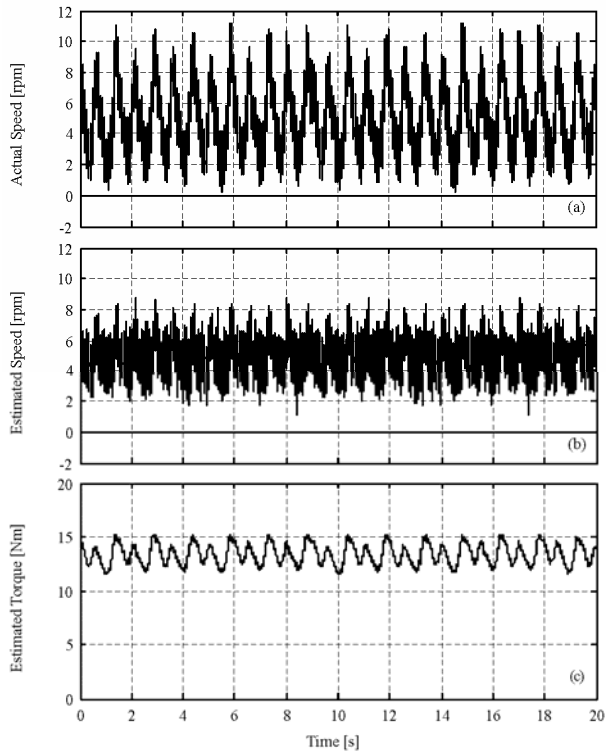

Figure 8. Stationary 5 rpm at 100% of nominal torque; from top to bottom: actual speed, estimated speed and estimated torque
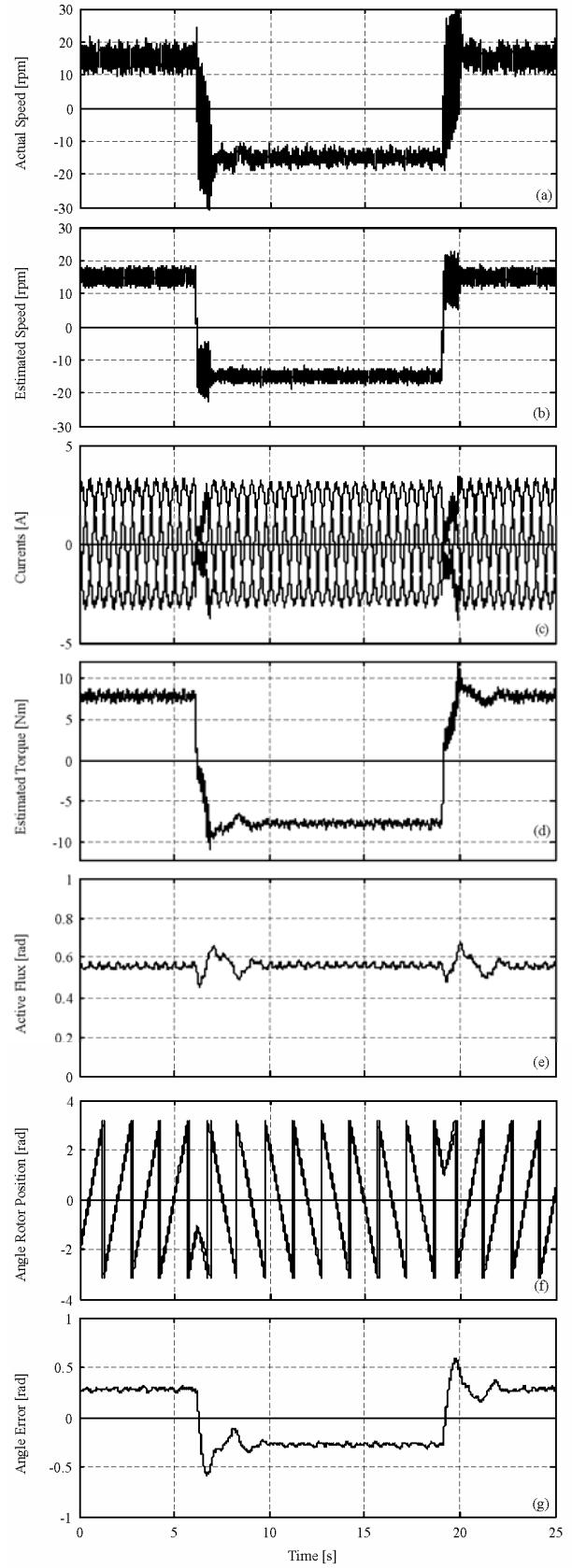

Figure 9. Speed reversal at ± 15 rpm and 50% of nominal torque; from top to bottom: actual speed, estimated speed, measured currents, estimated torque, active flux, angle rotor position (actual and estimated), error between estimated and actual angle rotor position
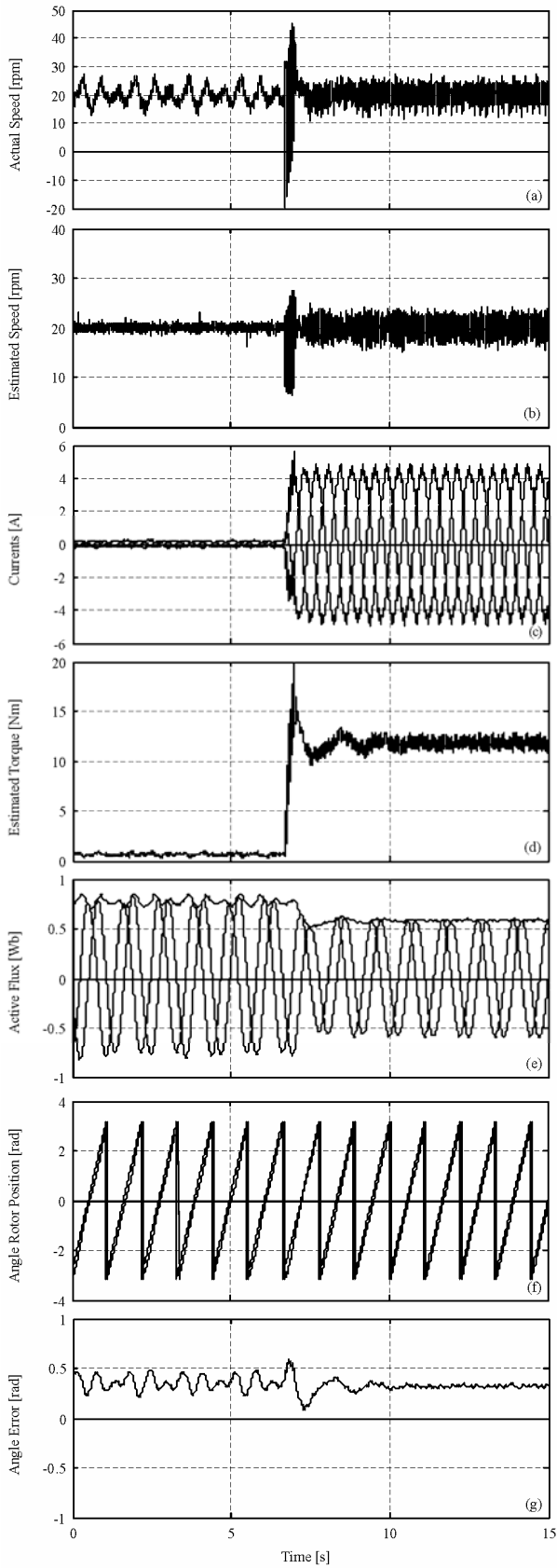
Figure 10. Torque transients at 20 rpm and full load; from top to bottom: actual speed, estimated speed, measured currents, estimated torque, active flux, angle rotor position (actual and estimated), error between estimated and actual angle rotor position
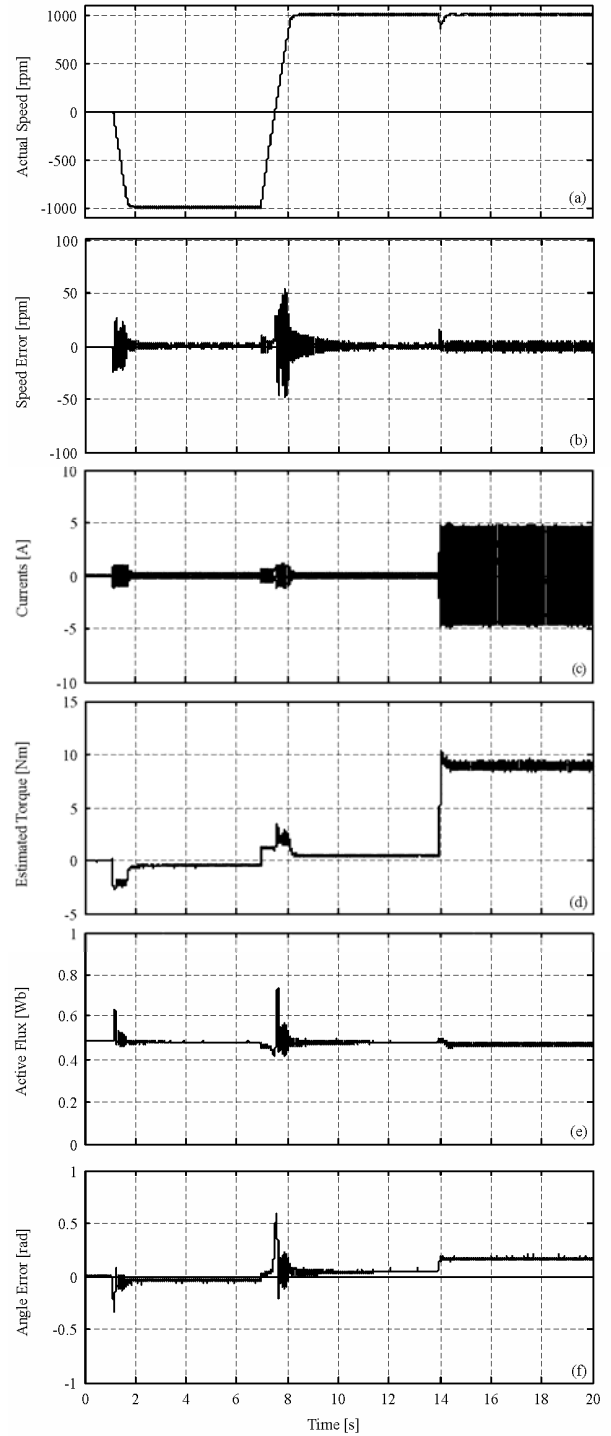

Figure 11. Startup response from 0 to -1000 rpm, speed reversal at ∓1000 rpm and torque transients at 1000 rpm at 60% of nominal torque; from top to bottom: actual speed, error between estimated and actual speed, measured currents, estimated torque, active flux, error between estimated and actual angle rotor position

At high speeds (Figure 11), the back electromotive force (EMF) will approach the available inverter voltage and can make proper current regulation difficult due to a lack of the necessary voltage margin, which explains the presence of spikes in the current (torque) waveforms.
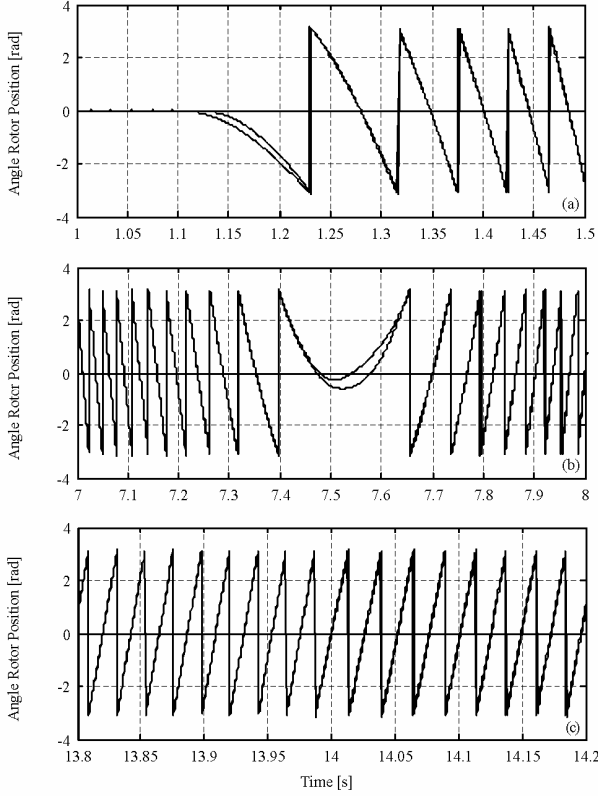
Figure 12. Start up response from 0 to -1000 rpm, speed reversal at ∓ 1000 rpm and torque transients at 1000 rpm at 60% of nominal torque; from top to bottom: actual angle rotor position at start up, at speed reversal and at step torque load
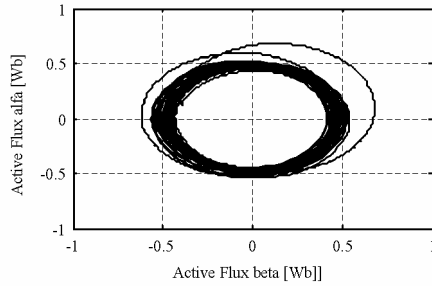

Figure 13. Start up response from 0 to -1000 rpm, speed reversal at ∓ 1000 rpm and torque transients at 1000 rpm at 50% of nominal torque: active flux beta versus active flux alfa hodograph

VI. CONCLUSION

This paper focuses on performance motion sensorless control of IPMSM via stator flux estimation using the "active flux" concept.

The current vector control strategy, using the proposed observer and without signal injection, was applied to the IPMSM sensorless drive in a speed range down to 2 rpm and up to 1000 rpm.

The experimental results show that the proposed state observer has been able to deliver accurate estimation both in steady state and during transients.

As the magnetic saliency is ignored in the state estimators, the proposed solution is a general approach that can be used in sensorless control of universal ac drives.

REFERENCES

[1] J. Holtz and J. Quan "Sensorless vector control of induction motors at very low speed using a nonlinear inverter model and parameter identification," *IEEE Trans. Ind. Appl.*, vol. 38, no. 4, pp. 1087–1095, July-Aug. 2002.

[2] S. Ostlund and M. Brokemper "Sensorless rotor-position detection from zero to rated speed for an integrated PM synchronous motor drive," *IEEE Trans. Ind. Appl.*, vol. 32, no. 5, pp. 1158-1165, Sept.-Oct. 1996.

[3] E. Urlep and K. Jezernik, "Low and zero speed sensorless control of nonsalient PMSM," in *Conf. Record IEEE-ISIE 2007*, pp. 2238–2243.

[4] C. Silva, G. M. Asher, and M. Sumner, "Hybrid rotor position observer for wide speed range sensorless PM motor drives including zero speed," *IEEE Trans. Ind. Electron.*, vol. 53, no. 2, pp. 373–378, 2006.

[5] A. Consoli, G. Scarcella, and A. Testa, "Industry applications of zero speed sensorless control techniques for PMSMs," *IEEE Trans. Ind. Appl.*, vol. 37, no. 2, pp. 513–521, 2001.

[6] G. D. Andreescu, C. I. Pitic, F. Blaabjerg, and I. Boldea, "Combined flux observer with signal injection enhancement for wide speed range sensorless DTFC of IPMSM drives," *IEEE Trans. Energy Convers.*, (to be published).

[7] I. Boldea, M. C. Paicu, and G. D. Andreescu, "Active flux concept for motion sensorless unified ac drives," *IEEE Trans. Power Electron.*, (to be published).

[8] I. Boldea, M. C. Paicu, G. D. Andreescu and F. Blaabjerg, "Active flux DTFC-SVM sensorless control of IPMSM," *IEEE Trans. Energy Convers.*, (to be published).

[9] M. W. Degner and R. D. Lorenz, "Using multiple saliencies for the estimation of flux, position and velocity in ac machines," *IEEE Trans. Ind. Appl.*, vol. 34, no. 5, pp. 1097–1104, 1998.

[10] F. Briz, M. W. Degner, P. Garcia, and R. D. Lorenz, "Comparison of saliency-based sensorless control techniques for ac machines," *IEEE Trans. Ind. Appl.*, vol. 40, no. 4, pp. 1007–1115, 2004.

[11] M. Linke, R. Kennel, and J. Holtz, "Sensorless speed and position control of synchronous machines using alternating carrier injection," in *Proc. IEEE-IEMDC-2003*, vol. 2, pp. 1211–1217.

[12] P. Garcia, F. Briz, D. Roca, and R. D. Lorenz, "Saliency-tracking-based sensor control neural networks," *IEEE Trans. Ind. Appl.*, vol. 40, no. 4, pp. 1007–1115, 2004.

[13] Y. Jeong, R. D. Lorenz, T. M. Jahns, and S. Sul, "Initial rotor position estimation of IPMSM using carrier frequency injection methods," in *Proc. IEEE-IEMDC-2003*, vol. 2, pp. 1218–1223.

[14] J.M. Guerrero, M. Leetmaa, F. Briz, A. Zamarron, and R.D. Lorenz "Inverter nonlinearity effects in high-frequency signal-injection-based sensorless control methods," *IEEE Trans. Ind. Appl.*, vol. 41, no. 2, pp. 618-626, March-April 2005.

[15] S. Ogasawara, H. Akagi "Implementation and position control performance of a position-sensorless IPM motor drive system based on magnetic saliency" IEEE Transactions on IA, vol. 34, Issue 4, July-Aug. 1998, pp. 806-812.

[16] Z. Chen, M. Tomita, S. Ishikawa, S. Dalhi, and S. Okuma, "Sensorless control of IPMSM by estimation of an extended emf," in *Conf. Record IEEE-IAS 2000*, vol. 3, pp. 1814–1819.

[17] S. Morimoto, K. Kawamoto, M. Sanada, and Y. Takeda, "Sensorless control strategy for salient pole PMSM based on extended emf in rotating reference frame," *IEEE Trans. Ind. Appl.*, vol. 38, no. 4, pp. 1054–1061, 2002.

[18] S. Morimoto, M. Sanada, and Y. Takeda, "Mechanical sensorless drives of IPMSM with online parameter identification," *IEEE Trans. Ind. Appl.*, vol. 42, no. 5, pp. 1241–1248, 2006.

[19] S. Koonlaboon and S. Sangwongwanich, "Sensorless control of IPMSM based on a fictitious PM flux model" in *Conf. Record IEEE-IAS 2005*, pp. 311–318.

[20] S. Shinnaka, "New mirror-phase vector control" for sensorless drive of PMSM with pole saliency," *IEEE Trans. Ind. Appl.*, vol. 40, no. 2, pp. 599–606, 2004.

[21] E. Roseischl and M. Schroedl, "Optimized INFORM measurement sequence for sensorless PMSM: drive with respect to minimum current distortion," *IEEE Trans. Ind. Appl.*, vol. 40, no. 2, pp. 591–598, 2004.